In Proceedings: *IEEE Int. Conf. on Robotics and Automation, Nice, France May 10-15, 1992, pp: 2178-2185*

Motion Constraints from Contact Geometry: Representation and Analysis*

Raju S. Mattikalli Pradeep K. Khosla
Engineering Design Research Center
and The Robotics Institute,
Carnegie Mellon University,
Pittsburgh, PA 15213.

Abstract

A method to determine constraints on translational and rotational motion of planar and 3-D objects from their contact geometry is presented. Translations are represented by spatial vectors and rotations by axes in space. For each of these, a geometric realization ($\mathcal{M}_a$) of the space of motion parameters is created. Subspaces in $\mathcal{M}_a$ that represent the range of values of motion parameters that are 'disallowed' due to the contact are identified. The geometric realization makes it easier to visualize results, provides a good measure of the extent of restraints between objects, reduces computations by eliminating redundant constraints, and simplifies computation of net constraints. The proposed representation can be used effectively to automate the evaluation of motion constraints.

1 Introduction

Automatic generation of high level assembly plans from computer models of assemblies has been an area of much research interest. Some approaches[1, 2, 3], are based on connectivity information and precedence knowledge to produce an *ordering* of components. Others[4, 5] adopt a more geometrically intensive approach, generating assembly motion plans from disassembly simulations. With a broader goal, our research[6, 7], and that of [8], is aimed at developing a system that creates assembly plans and real-time code directly from geometric models of an assembly. One of the important components of this system is a methodology to reason about motion constraints using the 3-D geometric modeler input description of an assembly.

In this paper,we present a method to determine motion constraints (both translational and rotational) on an object based on its contact geometry. Constraints due to individual mating surface elements are computed; these effects are then superposed to obtain the constraint due to the entire surface. A geometric realization of the space of all possible motion parameters ($\mathcal{M}_a$) is constructed. $\mathcal{M}_p$ is a subspace in $\mathcal{M}_a$ that represents all permissible motions ($\mathcal{M}_p \subseteq \mathcal{M}_a$). If the object has no mating surfaces, $\mathcal{M}_p = \mathcal{M}_a$. A mating surface element prevents the object from moving along a certain set of directions. The subspace over which motion is disallowed is referred to by $\mathcal{M}_d$. The knowledge of motion constraints produced by contact is required in various aspects of assembly planning - in determining degrees-of-freedom of components and subassemblies, in analyzing stability of subassemblies, planning grasps, synthesizing fixtures, etc. The representation and analysis of motion constraints presented in this paper can be used effectively in making these evaluations.

This paper is organized as follows. Section 2 describes some relevant work in the area of kinematic analysis of objects in contact and highlights the contributions made by this work. Section 3 and 4 describe the motion spaces and the computation of restraints for translational and rotational motion, respectively. The proposed analysis is applied to an example in section 5. Section 6 summarizes this paper and points out directions for future research.

2 Motion Constraints from Contact

Reuleaux[9] analyzed the effect of point contact on translational and rotational motion of planar objects.

*This research was supported in part by the Engineering Design Research Center, an NSF Engineering Research Center at Carnegie Mellon University

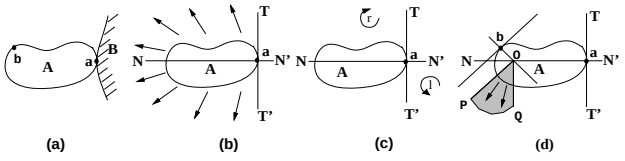

Figure 1: Reuleaux's analysis of restraints **(a)** A planar object A with contact at a, **(b)** Restraints to translations-directions between TN'T', **(c)** Restraints on anticlockwise (NTN') and clockwise (NT'N') rotation **(d)** Superposition-contact at a and b.

Using a graphical method, he derived the field of restraint (a set of directions in which motion is prevented) for a point contact. This method is shown in fig. 1 where the restraints on object A are derived. Consider contact point a. The normal at the point of contact defines the field of restraint on translation - in fig. 1(b) these are directions between $TN'T'$. Calculation of restraints for two points of contact (a and b) is shown in fig. 1(d). Directions in sector POQ (shown shaded) make up the net allowed directions for motion. The analysis of restraints against turning proceeds along similar lines and is shown in 1(c). Clockwise turning is permitted in the region above (and including) line NN' whereas anticlockwise turning is permitted in the region below (and including) line NN'.

[10] used configuration spaces to represent reachable configurations of objects. This is used to describe the kinematics of interacting objects. Ohwovoriole [11] used the theory of screws to study the kinematics of the relative motion of contacting bodies. In dealing with planar motion, Reuleaux's method is simpler than that of Ohwovoriole and provides identical results. Our method follows the lines of Reuleaux's method, extending it to spatial motions. Geometric representations of translational and rotational motion are proposed. These representations are more amenable to computer implementation and also lead to simplifications in analysis.

This paper makes three important contributions. First, it extends restraint analysis to 3-D objects, allowing for general translational and rotational motion. Second, the work presents an analysis of restraints not only from *point* contacts, but also from contact extending over *surfaces*. Points that define the boundaries of constraint regions are identified and used. Third, a compact geometric representation of the space of all possible translational and rotational axes is proposed. Constraints are represented as subspaces in the proposed space. This representation of constraints has a number of advantages over algebraic representations (such as equations 1 and 2). It is easier to visualize and interpret; redundancy among constraints can be easily identified; available geometric algorithms can be used. Moreover, some interesting properties of the space $\mathcal{M}_p$ are obtained as a result of employing the geometric representation. These lead to simplifications in the computer representation as well as superposition. This measure is used as a criterion in decomposing assemblies during disassembly planning.

The next section describes the geometric representation of the space of motion parameters for spatial translations.

3 Translational Degrees of Freedom

Given the geometry of contact between objects O_1 and O_2, the objective is **to find** directions along which O_1 possesses instantaneous translational motion relative to O_2. First, a representation of the space of all possible directions for translational motion is constructed. Then effect of each mating element on these directions is calculated.

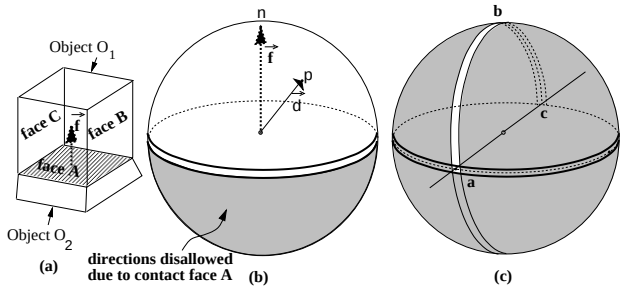

Figure 2: **(a)** An object (O_1) with its mating face (face A) shown shaded, **(b)** The direction sphere. Shown shaded are directions disallowed by mating face A. **(c)** Superposition - with mating on faces A, B and C.

Consider a sphere of unit radius (as shown in fig. 2(b)). Any arbitrary direction vector ($\vec{d}$) can be mapped onto a point (p) on the unit sphere. This mapping is bijective (on-to-one and onto) and can be used to represent all directions in $\Re^3$. Consider object O_1 (in fig. 2(a)) in contact with O_2 along face A with inward normal $\vec{f}$. Fig. 2(b) shows the directions that are "disallowed" as the shaded hemisphere on the direction sphere. This set of points is open (i.e. it does not include the great circle). If faces B and C were also mating faces, the net restraint would be as shown

in fig. 2(c). The object O_1 now possesses translational *dof*s only along directions represented by the arc *abc*.

An algebraic representation of a translational constraint is an inequality of the form

$$\vec{d}\,.\vec{n} \;\geq\; 0 \qquad (1)$$

where $\vec{d}$ is an allowed direction for translation, and $\vec{n}$ the inward normal of a face of contact. With m contact faces, m such inequalities would be obtained. Without a geometric representation, it is not easy to visualize the significance of each constraint nor their solution. Redundant constraints can be identified by constructing the convex hull of the inward normals of all the faces of contact. Normals that lie on the interior of this convex hull are redundant constraints. By intersecting hemispheres of adjacent vertices on the convex hull, the allowed region for translational motion can be obtained. With this geometric representation, superposition of two constraints (union of two hemispheres) can be got from a simple cross product of the two normals. Moreover, the area of the allowed region (in the case of fig. 2(c) the arc length *abc*) gives us the extent of restraint on an object. This could be used as a measure for selecting components in order to grasp/fixture assemblies - a component that provides a larger restraint on other components is a good candidate.

4 Rotational Degrees of Freedom

Given the geometry of contact between objects O_1 and O_2, **to find** axes about which O_1 possesses instantaneous rotational motion relative to O_2. An arbitrary rotational axis is defined by $(\vec{r}, \vec{\varphi})$, where $\vec{r}$ is a direction vector and $\vec{\varphi}$ the position vector of a point on a plane that is perpendicular to $\vec{r}$. The proposed method will be introduced by applying it to planar polygonal objects.

4.1 Rotational *dof*s for planar objects

Polygonal Objects : Consider a polygonal object O_1 in the XY plane (fig. 3(a)) which has mating constraints as shown. Let $(\vec{r}, \vec{\varphi})$ be an axis of rotation. For planar objects in the XY plane, $\vec{r}$ can be along either the $+Z$ or the $-Z$ directions. Thus two planes ($\mathcal{M}_a^+$ and $\mathcal{M}_a^-$, one for each direction of $\vec{r}$) can be used to represent $\mathcal{M}_a$, the space of all planar rotations. Consider the mating element on O_1 represented by edge E_a with inward normal $\vec{f}$.

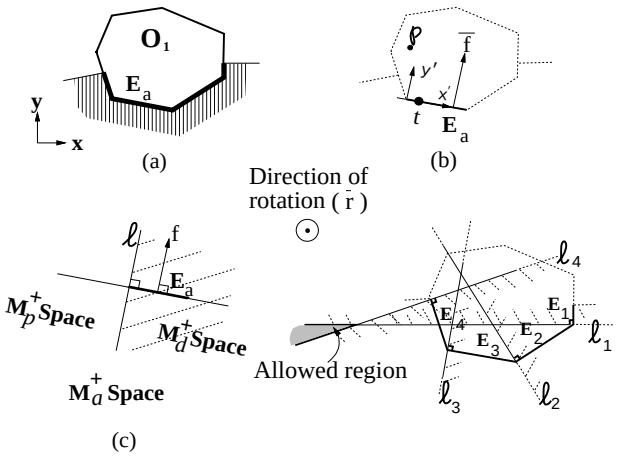

Figure 3: Rotational Restraints on planar objects **(a)** A polygon with its mating conditions, **(b)** A single mating element E_a, **(c)** Anticlockwise rotation is disallowed about axes that lie in the shaded region. **d** Superposition

To find rotational constraints due to E_a, consider fig. 3(b). Let t be an arbitrary point on E_a. The rotation $(\vec{r}, \vec{\varphi})$ is disallowed if

$$(\overline{r} \times \overline{\varphi t})\,.\,\overline{f} \;<\; 0 \qquad \forall\, t \in E_a \qquad (2)$$

which is the scalar triple product of the vectors $\overline{r}, \overline{\varphi t}$ and $\overline{f}$. When the above quantities are described with respect to the (x', y') frame (shown in figure 3(b)), we obtain

$$x \;>\; 0 \qquad (3)$$

In fig. 3(c), points in the right half plane of line ℓ (shown shaded) represent axes disallowed by the mating element E_a. Other mating edges impose similar restrictions on permissible axes of rotation. The union of all these subspaces (as shown in fig. 3(d) produces the subspace of disallowed axes $\mathcal{M}_d^+$. To obtain the permissible region, an algorithm of time complexity $\mathcal{O}(N \ln N)$, where N is the total number of constraints, is described in [12].

In this case again, the geometric realization allows easy identification of redundant constraints. In the next paragraph, we describe a method of identifying those constraints that define the boundary of the permissible subspace $\mathcal{M}_p$; the remaining constraints are redundant hence are ignored. The method is used to identify constraints due to planar objects bounded by curves.

General Planar Objects : For curved surfaces of contact, each point along the curve produces a half

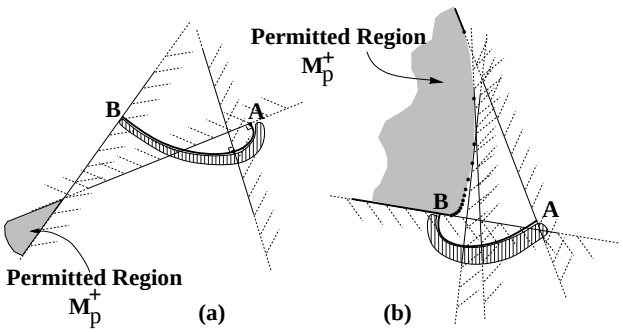

Figure 4: Contact over curves. **(a)**: Decreasing curvature along AB, **(b)** Increasing curvature along AB.

plane such as those in fig. 3(d). We identify segments of the contact curve that produce redundant constraints. To do so, the curve of contact is divided into segments where the curvature is either decreasing or increasing. Also divisions are made at points of inflexion. Segments of increasing and decreasing curvature are analyzed separately. Details of the analysis can be found in [13]. The following results are obtained which are shown in fig. 4.

Result 1: The constraints imposed by the endpoints of a segment with a non-increasing curvature make redundant the constraints imposed by points inbetween them.

Result 2: For segments of contact with increasing curvature, the constraints imposed by the end points along with the locus of centers of curvature of points between them are sufficient to define $\mathcal{M}_d$.

Thus by computing

1. constraints due to a limited set of contact points, and
2. the locus of centers of curvature over segments with decreasing curvature,

we can determine $\mathcal{M}_d$ due to curvilinear contact between planar objects.

In section (4.2) we extend this method to polyhedral objects. Some interesting properties of the representation emerge, which are explored. Superposition of the $\mathcal{M}_d$s due to each of the contact elements is a challenging problem and solutions to this problem are presented.

4.2 Rotational *dof*s for polyhedral objects

The method of analyzing rotational *dof*s for objects in $\Re^3$ is similar to that of analyzing planar objects. However, the geometric representation of the space $\mathcal{M}_a$ is more involved than that for planar objects. To represent an arbitrary axis in $\Re^3$, 4 independent scalars are required. In section (4.2.1) we present a representation that is geometrically realized. This realization is the key to the discovery of some important properties which lead to a compact computer representation of all possible axes of rotation. Subsequent analysis of rotational *dof*s is simplified as a result of compactness in the representation.

4.2.1 Tangent Plane Enhanced Direction Sphere

Consider the direction sphere as shown in fig. 2(b). Let the point n be the north pole of this sphere. Unit vector ($\vec{d}$) has its tail at the center of the sphere and its head on point p on the surface. Imagine placing a plane (T_p) tangential to the sphere at point p. Define a local frame of reference on T_p at the point of contact with the sphere, with its Z axis along $\vec{d}$ and its Y axis tangent to the longitude pointing north. An axis of rotation parallel to $\vec{d}$ can be represented by a point on T_p, expressed in terms of the local coordinate frame. If we construct planes tangential to all points on the sphere, we have a geometric representation for all possible axes of rotation, which will be referred to as the tangent plane enhanced direction sphere. This is the space $\mathcal{M}_a$ for objects in $\Re^3$. The set (θ, ϕ, x, y) is an algebraic representation of the same.

4.2.2 Constraints on Permissible Axes of Rotation due to a Planar Contact Face

Consider the object with a single planar contact surface as shown in fig. 2(a). The mating face is isolated and shown in fig. 5(a). $\vec{r}$ is parallel to the X axis; N is a plane normal to $\vec{r}$. An analysis of restraints on axes of rotation whose direction vector $\vec{d}$ is parallel to $\vec{r}$ is performed. Details can be found in [13]. The results are shown in 5(b). Line ℓ is perpendicular to the projection of the face *abcd* located at the left extreme of the projection. This line defines the bounds of the open set $\mathcal{M}_d$ which is shown hatched.

Constraints imposed by a face contact in other directions on the equatorial plane of the sphere are considered next. Consider the equatorial plane shown in fig. 6. Draw $\overline{OA}$,$\overline{OB}$, etc parallel to the edges of contact face *abcde*. Let m_a, n_a be the projection of the face *abcde* on the tangent plane T_a at point A. The line perpendicular to m_a, n_a on T_a is ℓ_a which defines the bounds of the constraint region on T_a. The same holds for the rest of point B through E. Constraints on tangent planes at points along AB is given by the

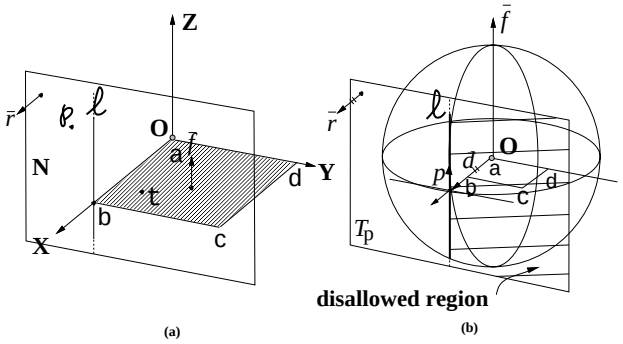

Figure 5: **(a)**:Analysis of restraints on rotation along $\vec{r}$ due to mating face $abcd$, **(b)** The space $\mathcal{M}_a$ showing the disallowed region $\mathcal{M}_d$ in the direction $\vec{d}$.

projection of a rotating vector Oa, rotating in a direction opposite to that from A to B.

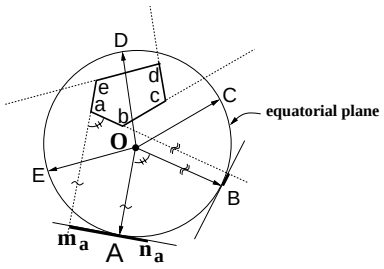

Figure 6: Variation of the constraints along the equator.

The influence of a contact face on directions other than those on the equator is stated in the following result (details in [13]).

Result 3 : All directions along a longitude (excluding the poles[1]) of the sphere have identical tangent planes due to a single contact face.

The invariance of ℓ along a longitude makes it sufficient for us to represent only those tangent planes that lie on the equator.

Another important property of the line ℓ is its invariance to translations of face $abcd$ in the direction of its normal. This is shown in [13].

To recapitulate some of the salient features,

1. We have developed a representation for the space of all rotational axes,
2. We have developed a method for constraining the space of rotational axes due to the presence of a single surface element,
3. We discovered a useful property: the invariance of ℓ over axes that have the same azimuth angle,
4. Another useful property, namely the invariance of ℓ with translations of the face of contact along a direction normal to the face, was also proved,
5. translations of the contact face within its plane requires the recomputation of ℓ.

The items (3) and (4) above are useful in superposing the constraints due to each contact face to get the rotational degrees-of-freedom of the part. In what follows, a solution to the problem of computing the net *dof* of a part by superposing individual constraint spheres is presented.

4.3 Superposition of Constraint Spheres

In section 4.2.2, constraints imposed by a single planar contact face on rotational motion was analyzed by constructing a sphere whose Z axis was aligned parallel to the normal of the face. For objects with multiple contact faces, constraint spheres (one for each face) that are aligned along their respective face normals are obtained. To calculate the net constraint at a point on the sphere, a method to superpose these constraint spheres is required. Let $\mathcal{S}_f$ be a constraint sphere oriented arbitrarily with respect to the global frame $\mathcal{S}_g$. The transformation of restraints captured in sphere $\mathcal{S}_f$ to sphere $\mathcal{S}_g$) is obtained as follows.

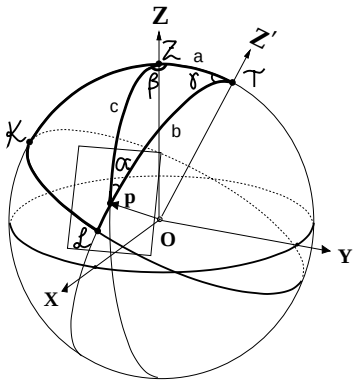

Figure 7: Construction to transform the restraints captured in a local sphere ($\mathcal{Z}'$) to the global sphere ($\mathcal{Z}$).

Refer to fig. 7. Frame XYZ is the global reference frame. The Z axis corresponding to point $\mathcal{Z}$ on the sphere $\mathcal{S}_g$. Let $X'Y'Z'$ be a reference frame attached to sphere $\mathcal{S}_f$. The Z' axis corresponds to point $\mathcal{T}$ on sphere $\mathcal{S}_g$. **Given** a point p in XYZ we want

[1] Thanks to one of the reviewers of this paper for pointing out the exception at the poles

to calculate the restraints on tangent plane T_p due to sphere $\mathcal{S}_f$. We know from section (4.2.2) that the restraints on T_p due to a single planar contact face is defined by a line ℓ. However ℓ is computed with respect to the local frame at p whose Y axis is aligned with the longitude $\mathcal{T}p$. A rotation of $-\alpha$ would give line ℓ with respect to a local frame at p whose Y axis is aligned with the longitude $\mathcal{Z}p$. Two quantities are required, namely (a) the location of point p with respect to the $X'Y'Z'$ axis, and (b) the angle α. $\mathcal{K}$ and $\mathcal{L}$ are the points of intersection of the great circle of $\mathcal{S}_f$ with longitudes that pass through points $\mathcal{Z}$ and p. From result 3 we can know that line ℓ with respect to the $X'Y'Z'$ is identical at points $\mathcal{L}$ and p. Thus $\ell(\mathcal{KL})$ would give the required location of point p. The following equations can be derived using spherical oblique triangle equations (details in [13]).

$$\alpha = X + Y, \ where \tag{4}$$

$$X = \tan^{-1} \frac{\cos(\beta/2)\ \cos[(a-c)/2]}{\sin(\beta/2)\cos[(a+c)/2]} \ and \tag{5}$$

$$Y = \tan^{-1} \frac{\cos(\beta/2)\ \sin[(a-c)/2]}{\sin(\beta/2)\sin[(a+c)/2]} \tag{6}$$

and

$$\ell(\mathcal{KL}) = \tan^{-1}(\sin b\ \tan\alpha) \tag{7}$$

In summary, we have shown is that for each face of contact, by storing

1. the geometry of the face,
2. the spherical coordinates of the normal of the face when represented on the global constraint sphere,
3. the partitioning of the equator of the constraint sphere of the face based on the regions 'governed' by a single vertex

the space of disallowed axes of rotation $\mathcal{M}_d$ (which is given by ℓ) due to that face can be computed. By transforming the half planes defined by the ℓs due to each of the contact faces to a global frame and then computing their intersection, the convex region that represents $\mathcal{M}_p^{net}$ can be obtained.

5 An example

Consider the assembly in fig. 8, which shows the housing of a fishing rod having three components A, B and C. We will apply the proposed method to calculate the restraint that object C imposes on object B. At the onset, it is worth noting that the only relative *dof* between the two object is a rotation about an axis parallel the the $+X$ axis passing though the center of the hinged joint H. The surfaces of contact between

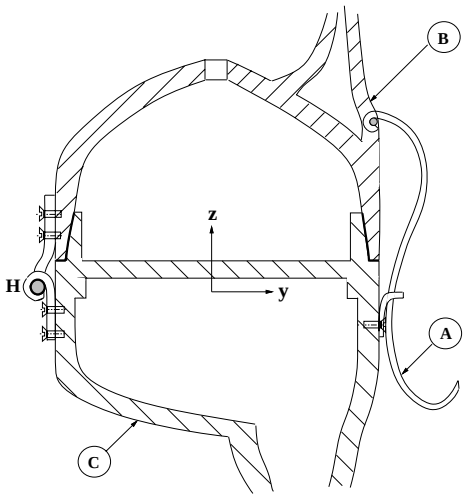

Figure 8: An example of an assembly. Of interest is the contact between objects B and C.

objects B and C are isolated and shown in fig. 9. Consider surface P in fig. 9(b) which is part of a sphere centered at O. Since surface P is symmetric about the axis $\overline{x_1x_2}$, restraints due to segment abc can be rotated and superposed to obtain the restraints due to the entire surface. Although the origin of the direction sphere can be placed at any point in space, with any orientation, for convenience, the origin is placed at O with its Z axis oriented along axis ($\overline{x_1x_2}$) and X axis along the outward normal of the page.

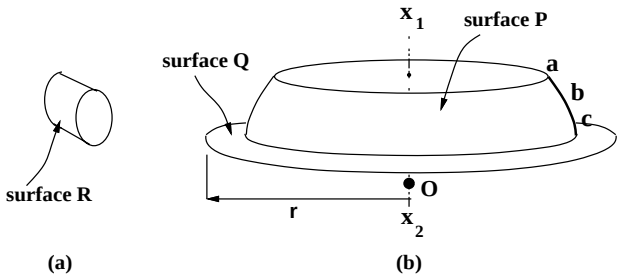

Figure 9: Contact surfaces between objects B and C.

Fig. 10 shows the calculation of translational constraints. The direction sphere in fig. 10(a) shows shaded the directions which are 'disallowed' by segment abc. This region when rotated about the Z axis produced the direction sphere in fig. 10(b) which gives

the net restraint on translation due to surface P. Direction spheres due to surface Q (fig. 10(d)) and surface R (fig. 10(e)) are also calculated. The net direction sphere due to all three contact surfaces is obtained by taking a union of the 'disallowed' regions due to each of the surfaces and is shown in fig. 10(f). This shows that contact constraints do not permit any translational motion between objects B and C.

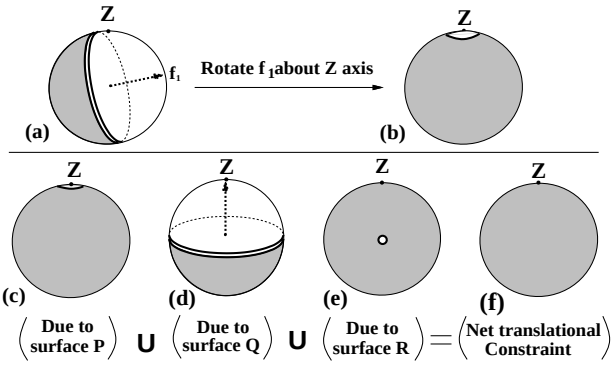

Figure 10: Translational constraints on object B by object C.

The analysis for rotational constraints due to surface P is shown in fig. 11. Fig. 11(a) shows the direction sphere, with surface P superimposed for convenience. Since we know that the net *dof* will exist on a tangent plane whose normal is the $+X$ direction, we will focus on that plane (referred to as T_p^A). The solution method consists of determining the constraints on T_p^A due to segment abc, followed by other segments sequentially so as to cover the entire surface. In order to help explain the progressive addition of constraints on T_p^A, we shall make use of the symmetry of the surface. Since surface P is symmetric about the Z axis, tangent planes on all points on the great circle $ABCD$ will be identical. The effect of segment abc along all points on the great circle $ABCD$ are analyzed. If these solutions are superimposed, then the solution will be identical to analyzing the effect of the entire surface at the single point A. The effect of the differential area f_1 at points A, B, C and D is shown in the first row of fig. 11(b). Each constraint region is determined using the method described in section 4.2.2. Note that the boundary of the constraint due to f_1 at A can be easily verified by projecting the normal at f_1 onto the tangent plane at A. Similar projections on the tangent planes at B, C and D can be used to verify the other constraint boundaries in the first row. Note that as we traverse the great circle from A to B and so on back to A, the boundary of the constraint region rotates about the point O from one maximum position at A to the other at C and then back. Similar analysis is carried out to find the constraints due to f_2 (along row 2) as well as f_3 (row 3). Examine the variation of constraints along a single column - the variation at a given point due to different points along segment abc. Again, the points corresponding to f_1 and f_3 define the bounds; all other constraints are included within these. The union of the 'disallowed' regions along a column gives the net constraint at a given point due the segment abc. The union of the regions at the four points gives the net constraint at any point on the great circle due to surface P. This is shown if fig. 11(c).

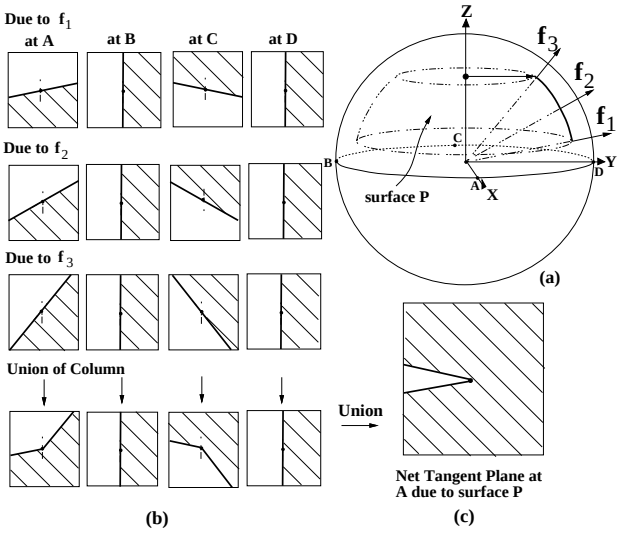

Figure 11: Calculation of rotational constraints on object B due to surface P.

The constraints due the surface Q and surface R are obtained in a similar manner and are shown in fig. 12(b) and 12(c). The net rotational constraint at point A to to all three surfaces is obtained by taking the union of each of the 'disallowed' regions. We can see in fig. 12(d) that the *dof* which object B possesses is along a single point on T_p^A. It can be shown that there is no other tangent plane that possesses a *dof*.

The discussion in this paper, did not include an analysis of constraints for curved surfaces (although we were able to demonstrate an example using simple curved surfaces). The method is identical to that discussed for polyhedral contact surfaces. In order to implement the method on a computer, only finitely many tangent planes can be represented. Tangent planes at other locations can be derived from these. For each planar face, a sphere with its north pole in the direc-

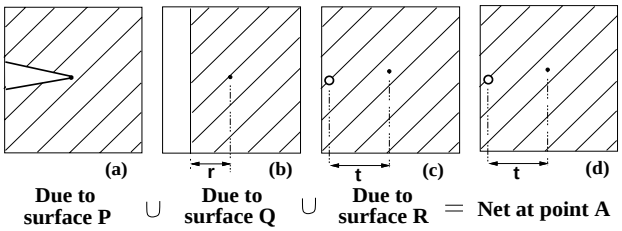

Figure 12: Net rotational constraints on object B.

tion of the face normal is constructed; each such sphere has finitely many tangent planes of interest. For polyhedral objects, due to superposition, tangent planes of interest can easily be determined. However, for curved surfaces, the location of these tangent planes is not obvious. A study of the variation of constraint regions due to curved surfaces is required. It is expected that results similar to those obtained for curved lines (section 4.1) will be obtained. This would allow us to use finitely many tangent planes to construct a complete representation of constraints due to curved surfaces.

6 Summary and Future Directions

A method for calculating and representing restraints on components due to contact with other components has been presented. Translational and rotational restraints are represented separately. A geometric representation of the space of all possible motion parameters is constructed. The restraints imposed by a single mating surface element is analyzed by a determining portions within this space that are 'disallowed'. By computing the union of the disallowed regions due to each contact surface element, and taking its complement with respect to the whole space, the space of allowed motion parameters is obtained. Objects in both $\Re^2$ as well as $\Re^3$ are analyzed.

The knowledge of restraints plays a fundamental role in the simulation of assembly. To produce an assembly plan, we simulate a disassembly of the design. Selection of subassemblies uses knowledge of restraints in finding subassemblies that possess degrees-of-freedom. Also, restraints are used to suggest initial motions for disassembly. The method of reasoning requires a mechanism for selection of subassemblies based on *stability* among the components in the assembly. Stability can be inferred from knowledge about restraints due to contact. We believe that the representation of restraints that is proposed in this paper is an important step towards automated assembly planning and analysis.

References

[1] K. Lee and H. Ko, "Automatic assembly procedure generation from mating conditions," *CAD*, vol. 19, no. 1, pp. 3–10, 1987.

[2] D. Whitney and T. DeFazio, "Simplified generation of all mechanical sequences," *IEEE Journal of Robotics and Automation*, vol. RA-3, no. 6, December, 1987.

[3] L. H. de Mello and A. Sanderson, "Representations for assembly sequences," in *Computer-Aided Mechanical Assembly Planning* (L. H. de Mello and S. Lee, eds.), pp. 129–162, Kluwer Academic Publishers, 1991.

[4] S. Sedas and S. Talukdar, "Disassembly expert," *Technical Report, Engineering Design Research Center, Carnegie Mellon University*, vol. EDRC-01-03-87, 1987.

[5] R. Hoffman, "Automated assembly in a csg domain," *Proc. IEEE Conference on Robotics and Automation*, pp. 210–215, 1989.

[6] R. Mattikalli, P. Khosla, and Y. Xu, "Subassembly identification and motion generation for assembly: A geometrical approach," in *Proceedings of IEEE Conference on System Engineering*, pp. 399–403, 1990.

[7] P. K. Khosla and et. al., "'cmu' rapid assembly system," *(to appear) in Proc. IEEE Int. Conf. on Robotics and Automation, Nice, France*, May, 10-15 1992.

[8] D. Strip and A. A. Maciejewski, "Archimedes: An experiment in automating mechanical assembly," in *Proc. Int. Symposium on Robotics and Automation, Vancouver*, July 18 1990.

[9] F. Reuleaux, *The Kinematics of Machinery.* Macmillan 1876, Republished by Dover, 1963.

[10] R. C. Brost, *Analysis and Planning of Planar Manipulation Tasks, CMU-CS-91-149.* PhD thesis, Carnegie Mellon University, January 1991.

[11] M. S. Ohwovoriole, *An extension of screw theory and its application to the automation of industrial assemblies.* PhD thesis, Stanford University, PhD Thesis, April 1980.

[12] F. P. Preparata and M. I. Shamos, *Computational geometry : an introduction.* New York: Springer-Verlag, 1985.

[13] R. S. Mattikalli and P. K. Khosla, "Analysis of restraints to translational and rotational motion from the geometry of contact," in *Proceedings of ASME Winter Annual Meeting, DE-Vol.39*, pp. 65–71, ASME, December 1991.